HYDROLOGICAL RESPONSE TO CLIMATE VARIABILITY AT DIFFERENT TIME SCALES: A STUDY IN THE EBRO BASIN

J.I. López-Moreno[1], S.M. Vicente-Serrano[1], J. Zabalza[1], S. Beguería[2], J. Lorenzo-Lacruz[1], C. Azorin-Molina[1], E. Morán-Tejeda[1].

1- Instituto Pirenaico de Ecología, CSIC (Spanish Research Council). Campus de Aula Dei. Zaragoza 50.059. Spain.

2- Estación Experimental de Aula Dei, CSIC (Spanish Research Council). Campus de Aula Dei. Zaragoza 50.059. Spain.

SUMMARY

In this study we analyzed the response of monthly runoff to precedent climatic conditions at temporal scales of 1 to 48 months in 88 catchments of the Ebro basin (northeast Spain). The standardized precipitation evapotranspiration index (SPEI) was used to summarize the climatic conditions at different time scales, and was correlated with the standardized streamflow index (SSI) calculated at the mouth of each catchment. The Ebro basin encompasses a gradient from Atlantic to Mediterranean climates, and has remarkable complexity in topography, geology and land cover. The basin is highly regulated by dams, which were built to produce hydropower and supply water for agriculture. These characteristics explain why sub-basins of the Ebro River basin respond in differing ways to precedent climatic conditions. Three main sub-basin groups were distinguished on the basis of the correlation of their streamflow responses to different time scales of the SPEI: (1) sub-basins correlated with short SPEI time scales (2–4 months), which generally corresponded to unregulated headwater areas; (2) sub-basins correlated with long SPEI time scales (10–20 months), where groundwater reserves play a major hydrological role; and (3) sub-basins correlated with medium

SPEI time scales (6–10 months). The latter occur in the lower sectors of the Ebro basin and its tributaries, which receive river flows from the other two sub-basins, and where dam regulation has a significant influence on the hydrological characteristics. In addition to the three main sub-basin groups, other streamflow responses associated with seasonal factors were identified, particularly those related to snowpack and the various management strategies applied to reservoirs.

Key words: time scales, times of response, standardized precipitation evapotranspiration index (SPEI), standardized streamflow index (SSI), dams, snow, Ebro basin

1. INTRODUCTION

Streamflow is an integrated response to basin inputs (climate), water transfer, water losses by evapotranspiration storage processes, and the effects of human activities on natural water flows. Prior to reaching the stream network a large proportion of precipitation is stored in various hydrological subsystems (including snowpack, soil moisture, groundwater reserves, reservoir storages) that respond to climatic conditions at different time scales (Vicente-Serrano and López-Moreno, 2005; McGuire and McDonnell, 2006). The results of previous research have shown that the catchment response time to precedent climatic conditions is highly variable among regions, as it depends of the physical attributes of the catchments (geology, topography, soils and vegetation), climatic conditions (evapotranspiration rates, snow cover, rainfall intensity) and dam operations (Post and Jakeman, 1996; Soulsby et al., 2006; Lorenzo-Lacruz et al., 2010; McDonnell et al., 2010; Fleig et al., 2011). The hydrological response to climate has also been shown to be seasonally dependent because the relative effects of

different water sources, climatic conditions, hydrological processes and water management vary throughout the water year (Tallaksen, 1995; García-Ruiz et al., 2008). For instance, in the Pyrenees it has been found that a 42% of the spring runoff are explained by the climatic conditions that occurred during winter (López-Moreno and García-Ruiz, 2004). It has also been demonstrated that water released downstream of dams will largely depend on the storage levels required at various times of the year. For example, the amount of water released during autumn from reservoirs built to supply water for agriculture during the dry season (late spring and summer) depends on the amount of water remaining at the end of the irrigation period (late September), while the releases in winter depend on the magnitude of inflows during autumn. In such cases the downstream flows show a much more marked response to climate at long time scales than at shorter ones (García-Ruiz et al., 2011). The maintenance of ecological flows during summer explains why no correlations are found between climatic conditions and river flows in most regulated rivers (i.e. López-Moreno et al., 2004). Other sources of seasonal variability are associated with the different characteristics of the recession curves during the year. Thus, Tallaksen (1995) found that steeper recession curves are generally typical of the summer period, especially in areas with shallow groundwater tables and extensive vegetation. This has been confirmed in small catchments in mountainous areas, where Hortonian flows dominate the runoff generation processes during summer and early autumn, in contrast with the remainder of the year when most of the surface runoff results from saturation excess processes and lateral runoff (García-Ruiz et al., 2008; Latron and Gallart, 2008)

The spatial and seasonal variability in the patterns of water storage and residence time make it difficult to identify scale-invariant climatic controls on runoff generation (Beven, 2002). For this reason it is important to analyze the response of river flows to

climate at various time scales. Advances in this field are necessary to improve the assessment and short-term forecasting of water resource availability, to better understand how river flows have reacted to past climatic trends and predict their response to various climate change scenarios.

The main objective of this study was to analyze the response of monthly runoff to precedent climatic conditions at various temporal scales (1–48 months). The study included 88 catchments of the Ebro basin (northeast Spain). For this purpose we used the standardized precipitation evapotranspiration index (SPEI; Vicente-Serrano et al., 2010), which has been used to summarize climatic conditions at various time scales and has been shown to have the capacity to explain temporal fluctuations in hydrological series in differing environments (Lorenzo-Lacruz et al., 2010). We investigated the main explanatory time scales of the SPEI for different months and sub-basins, and assessed spatial variability in the climate–runoff relationships. This involved correlation of the SPEI (calculated for 1–48 months) with monthly anomalies of river flows, quantified using the standardized streamflow index (SSI; Vicente-Serrano et al., 2011). The correlations were conducted for continuous series from October 1950 to September 2007, but also separately for each month. The curves that relate the change in correlation coefficient with the various time scales of the SPEI were used to assess the response time of each sub-basin to antecedent climatic conditions. The shapes of these curves were objectively classified to discriminate areas with a common hydrological response time.

The study represents a novel approach to analysis of the response time of river flow conditions to precedent climatic conditions at the basin scale. The Ebro basin is an excellent site for such research. It encompasses a gradient from Atlantic to

Mediterranean climatic conditions, and has remarkable complexity in topography, geology and land cover. The basin is highly regulated by dams that were built to produce hydropower and supply water for agriculture. In addition, the high density of gauging stations facilitates analysis of the hydrological response time to climate in undisturbed headwater areas, and aggregation of the effect of reservoir operations on the runoff response time in downstream sectors of the river.

2. STUDY AREA

The study area comprises approximately 83,000 km^2 in northeast Spain. The relief of the basin is very contrasted. The main unit is the Ebro valley, a depression through which the Ebro River runs. The valley is surrounded to the north and south by high mountain ranges that drain major tributaries (Fig. 1). The valley is enclosed to the north by the Cantabrian Range and the Pyrenees (maximum altitudes > 2000 and 3000 m a.s.l., respectively) and to the south by the Iberian Mountains (maximum altitude 2000–2300 m a.s.l.), while to the east and parallel to the Mediterranean coast the valley is sharply enclosed by the Coastal Range (maximum altitude 1000–1200 m a.s.l.).

The heterogeneous topography, contrasting influences of Atlantic and Mediterranean conditions, and the influence of various large scale atmospheric patterns (Vicente-Serrano and López-Moreno, 2005) generate an irregular distribution of climate parameters and variability in precipitation and temperature throughout the region (Ninyerola et al., 2007). Thus, long-term mean annual precipitation varies from 307 to 2451 mm yr^{-1}between different sub-regions of the basin. The centre of the Ebro basin is the driest sector, whereas the most humid areas are found in the Pyrenees and in the atlantic headwaters (West of the Ebro basin). Autumn and spring receives most of

precipitation (García-Ruiz et al., 2001The summer is relatively dry (with occasional rainstorms), as is the winter, when extended periods of anticyclonic conditions occur. However, in the westernmost part of the study area the winters are more humid because of continuous exposure to the passage of Atlantic fronts. The long-term average annual temperature varies from 0.8 to 16.2ºC. Elevation in the basin explains most of the spatial differences in temperature.

The contrasting topography and climatic characteristics within the basin explain the high variability of the river regimes among different sub-basins. Figure 2 shows marked differences in the long-term (1950–2005) monthly runoff measured at six gauging stations located in different parts of the study area. This shows that in general high flows are recorded in winter or spring, whilst summer produces the lowest discharges. Peak flows in spring are recorded mainly in the Jaca and Collegats rivers (Pyrenees), whereas maximum flows in winter are observed in those areas where snow plays a minor role (Daroca) or the climate is dominated by Atlantic influences (the Ebro River in Miranda de Ebro). Downstream sectors of the Ebro basin (Zaragoza and Tortosa) also have maximum river flows during winter, but they maintain substantial discharge during spring as a consequence of the contribution of Pyrenean tributaries and water stored in large reservoirs. Summer flows are relatively high in areas of Atlantic climate (i.e. the Ebro River in Miranda de Ebro) or in the basins where groundwater makes a significant contribution to total runoff, as occurs in the Jiloca River in Daroca.

The humid conditions of the mountainous areas, especially the Pyrenees, are in stark contrast to the dry characteristics of large areas of the Ebro River valley, emphasizing the importance of mountains in the hydrology and water resources of the entire basin (López-Moreno et al., 2011). The relative abundance of water in the area led to the

construction of numerous dams to regulate the main rivers, and this has caused major alterations to river regimes and reduced flood occurrences (López-Moreno et al., 2004).

3. DATA AND METHODS

The present study involved calculation of Pearson´s coefficients between long-term monthly river discharge series in different catchments of the Ebro basin with an index that represented the climate variability of each drainage area, determined at various time scales. Climatic data was provided by the Spanish Meteorological Agency (AEMET). Monthly series of precipitation (429) and temperature (55) were used. Observatories are located within the Ebro basin or in its immediate surroundings. The climate series were obtained from an original dataset of 1583 observatories through a process that included reconstruction, gap filling (only series with a maximum of 5% of missing data; they were filled using linear regression with neighboring stations which exhibited a correlation $r>0.9$), quality control and homogenization testing with independent reference series (see González-Hidalgo et al., 2009; Kenawy et al., in press). River flow evolution was analyzed at 88 gauging stations managed by the Ebro River Hydrographic Administration (Confederación Hidrográfica del Ebro, CHE). As for climatic data, hydrologic observations are evenly distributed across the entire Ebro basin (Fig. 1).

To assess the evolution of temperature and precipitation in a spatially-distributed fashion, monthly distributed layers from 1950 to 2006 at 1 km^2 resolution were created by interpolating values from the observatories, as described by López-Moreno et al. (2011). This was achieved using multiple linear regressions in which different geographic (latitude and distance to the Mediterranean Sea and the Atlantic Ocean) and

topographic (altitude) variables were used as predictors of monthly maximum and minimum temperature and precipitation (Daly et al., 1994). The residuals (the difference between the climatic variable measured at each weather station and the value predicted by the model) were subsequently determined for each observatory and interpolated over the entire area using local techniques (Ninyerola et al., 2007). The average temperature and precipitation in the sub-basins draining to each gauging station were averaged and used to calculate the SPEI.

The SPEI is based on a monthly climate water balance (precipitation minus potential evapotranspiration, PET), which is calculated at different time scales. The balances are then converted to standardized units to allow spatial and temporal comparisons. For this purpose the data is fit to a three-parameter log-logistic distribution. Calculation of the index follows a similar approach to that for the standardized precipitation index (SPI) (McKee et al., 1993 and 1995).

Once PET is calculated, the difference between the precipitation (P) and PET for the month i is calculated according to:

$$D_i = P_i\text{-}PET_i,$$

The calculated D_i values are aggregated at different time scales, following the same procedure as that for the SPI. The difference $D_{i,j}^k$ in a given month j and year i depends on the chosen time scale, k. For example, the accumulated difference for one month in a particular year, i with a 12-month time scale is calculated according to:

$$X_{i,j}^k = \sum_{l=13-k+j}^{12} D_{i-1,l} + \sum_{l=1}^{j} D_{i,l} \text{ , if } j < k, \text{ and}$$

$$X_{i,j}^k = \sum_{l=j-k+1}^{j} D_{i,l} \text{ , if } j \geq k,$$

where $D_{i,l}$ is the P–PET difference in the lst month of year i, in mm.

A three parameter distribution is needed to calculate the SPEI, since in two parameter distributions the variable (x) has a lower boundary of zero ($0 > x < \infty$), whereas in three parameter distributions x can take values in the range ($\gamma > x < \infty$, where γ is the parameter of origin of the distribution); consequently, x can have negative values, which are common in D series (Vicente-Serrano et al., 2010).

Using L-moment ratio diagrams, we tested the most suitable distribution to model the D_i values calculated at different time scales (Hosking, 1990). L-moments are analogous to conventional central moments, but are able to characterize a wider range of distribution functions, and are more robust in relation to outliers in the data. To create the L-moment ratio diagrams, L-moment ratios (L-skewness, τ_3; and L-kurtosis, τ_4) must be calculated. τ_3 and τ_4 are calculated as follows:

$$\tau_3 = \frac{\lambda_3}{\lambda_2}$$

$$\tau_4 = \frac{\lambda_4}{\lambda_2},$$

where λ_2, λ_3 and λ_4 are the L-moments of the D series, obtained from probability-weighted moments (PWMs) using the formulae:

$$\lambda_1 = w_0$$

$$\lambda_2 = w_0 - 2w_1$$

$$\lambda_3 = w_0 - 6w_1 + 6w_2$$

$$\lambda_4 = w_0 - 12w_1 + 30w_2 - 20w_3$$

The PWMs of order *s* are calculated as:

$$w_s = \frac{1}{N}\sum_{i=1}^{N}(1-F_i)^s D_i ,$$

where F_i is a frequency estimator calculated following the approach of Hosking (1990):

$$F_i = \frac{i-0.35}{N},$$

where *i* is the range of observations arranged in increasing order, and N is the number of data points.A full description of the methodology and validation is described by Vicente-Serrano et al. (2010). The SPEI is mathematically similar to the SPI, but it includes the role of potential evapotranspiration, which is calculated using the Thornthwaite equation (Thornthwaite, 1948). Recent research has shown that the method for determining the potential evapotranspiration does not affect the final output from this kind of index (Dai, 2011; van der Schrier et al., 2011).

The series of monthly discharge were converted to standard units through calculation of the standardized streamflow index (SSI; Vicente-Serrano et al., 2011). The SSI assumes that monthly river discharge series do not follow a normal distribution, and that the most appropriate frequency distribution is very likely to change among river sections and months of the year. The ability of six different three-parameter distributions (log-normal, Pearson type III, log-logistic, General Extreme Value, Generalized Pareto and Weibull) to fit any streamflow series was compared, and the most suitable distribution was selected according to the minimum orthogonal distance (MD) between the sample L-moments at site *i* and the L-moment relationship for a specific distribution (following Kroll and Vogel, 2002). Therefore, to obtain the *F(x)* for each monthly streamflow series we selected the probability distribution that showed the smallest D statistic, being common to select different probability distributions in the 12 monthly streamflow series

of a given station. Once the *F(x)* is calculated, the SSI (in z-scores) can easily be obtained, for example, following the classical approximation of Abramowitz and Stegun (1965):

$$SSI = W - \frac{C_0 + C_1 W + C_2 W^2}{1 + d_1 W + d_2 W^2 + d_3 W^3},$$

where

$$W = \sqrt{-2\ln(P)} \text{ for } P \leq 0.5,$$

and P is the probability of exceeding a determined x value, $P = 1 - F(x)$. If $P > 0.5$, P is replaced by $1-P$ and the sign of the resultant SSI is reversed. The constants are: $C_0 = 2.515517$, $C_1 = 0.802853$, $C_2 = 0.010328$, $d_1 = 1.432788$, $d_2 = 0.189269$, $d_3 = 0.001308$. If the distribution of probability is suitable to fit the different streamflow monthly series, the average value of the SSI must be 0, and the standard deviation 1. The SSI is a standardized variable, and it can therefore be compared with other SSI values over time and space.

It has been shown that the SSI provides for accurate spatial and temporal comparisons of the hydrological conditions in streamflow series in the Ebro basin (Vicente-Serrano et al., 2011). For example, Figure 3 shows the SSI corresponding to the Ebro River at the Zaragoza gauging station, and the SPEI calculated at time scales of 1, 6, 12 and 24 months for the drainage area of that gauging station between 1950 and 2005. The SPEI series has oscillations of a greater temporal frequency because the time scales are shorter, whereas at longer time scales the SPEI exhibits a lower frequency, enabling the detection of persistent dry and humid periods. A visual inspection of the SSI series

shows that at this gauging station the evolution of river flow anomalies occurred with intermediate temporal frequency (1–6 months).

To accurately assess the best SPEI time scale to explain the temporal variability in the streamflow series, we performed a correlation analysis between the SSI and the SPEI series at time scales from 1 to 48 months for each of the 88 sub-basins. The correlation analyses were conducted using the continuous SSI and SPEI series from October 1950 to September 2006, but we also performed independent analyses for each month to assess whether the relationships changed seasonally. Figure 4 shows a representative example of the correlation between the SSI series for the Jiloca and Veral rivers (in Daroca and Zuriza, respectively) with the SPEI calculated for time scales of 1–24 months. In Figure 4A the r-values correspond to the continuous SPEI series (from January 1950 to December 2005), and show that each basin correlated very differently to the SPEI time scales. The correlations show that the Jiloca River had a small response at short time scales but that this progressively increased, with maximum r-values occurring at time scales longer than 12 months. In contrast, the flow of the Zuriza River was highly correlated with the SPEI calculated at short time scales (2–4 months), but there was a rapid decrease in the correlation coefficients at longer time scales. This indicates that the Veral River has a much faster response to climatic conditions than the Jiloca River.

Figure 4B, which shows analyses for the monthly series of October, January, April and July, indicates that the patterns of SSI–SPEI correlations can change seasonally as a function of the SPEI time scale. Thus, for the Jiloca River in April the correlation coefficients tended to decrease slightly as the time scale increased, whereas in January the correlation coefficients increased continuously with increasing SPEI time scale. For

the Veral River the correlation coefficients changed in magnitude as a function of the month, with the greatest correlations occurring in July and the lowest r-values in January. Moreover, the decrease in the response of the SSI to the SPEI calculated for longer time scales was slower in October than in the other months. To summarize the correlations for each month we prepared contour plots for each basin (Fig. 4C), which enable rapid visual assessment of seasonal changes in the response time of each basin. This showed that the Jiloca River (Daroca) responded to relatively short time scales during spring and early summer, whereas from October to February the response time became progressively longer. The Zuriza River responded to short and medium time scales during autumn and winter, whereas in April and May the response time is lagged a few months as a consequence of the contribution from the melting of snow, which accumulated during the previous months.

A principal component analysis (PCA) classified the 88 sub-basins of the Ebro River on the basis of similarities of the correlations between the continuous SSI series and the SPEI at different time scales; and also according to the differing patterns of correlation at the monthly basis. This classification involved a PCA in S mode to identify general patterns in correlations of the SSI with various SPEI time scales. This mode establishes loading values that correspond to each pattern and can be transformed to exact scores, which can then be presented spatially to determine their spatial representativeness. PCAs were performed for the continuous and the monthly series, respectively. The PCA for the former was conducted with respect to the time scale of 1 to 48 months, and the latter was conducted with respect to variations in r-values for time scales spanning 1 to 24 months in benefit of a major resolution for the time-scales when more response in correlation exists. For the PCAs we selected a correlation matrix. The number of components was chosen on the basis that any new component included should explain

at least 5% of the total variance. The components were rotated to redistribute the final explained variance and to obtain more stable, physically robust patterns (Richman, 1986). To achieve this we used a Varimax rotation, which is the most widely applied approach because it provides clearer and physically explainable patterns (Jolliffe, 1990). Each sub-basin was grouped according to two classifications: one for the continuous series and one for the monthly correlations. The classification was based on the PCA loadings, following the maximum loading rule.

4. RESULTS

4.1 Correlation of the continuous SSI and SPEI series

Continuous correlations between the SPI and SSI series enabled a general picture of the response time of each sub-basin to antecedent climatic conditions of 1 to 48 months to be obtained. Three components summarized the different r-value curves for the basin, and explained 95% of the total variance. Figure 5 shows the three curves that represent each of the discriminated patterns, and Figure 6 shows the factorial loadings of each sub-basin. Principal component 1 (PC1) represents those sub-basins that mainly responded at short SPEI time scales (maximum response at a time scale of 2 months). The correlation coefficients between the SSI and the climatic water balance declined very rapidly for medium and long time scales. This pattern explained 63% of the total variance and was representative of large areas of the westernmost part of the Ebro River and headwaters of the western and central Pyrenees. It is noteworthy that three sub-basins exhibited strong negative PCA loadings with PC1, indicating the presence of a fourth pattern in the basin that mirrors PC1, with very low correlations at short time scales and a large response of the SSI to very long time scales of the SPEI. Similarly,

component 2 (PC2; 21% of the total variance) represents a pattern characterized by low correlations between the SSI and the SPEI at short time scales (1–3 months), and a continuous increase in the correlation to time scales of 15–20 months, when the maximum response of the SSI to the SPEI occurred. The correlation coefficients decreased slowly after month 20, but statistically significant correlations were still evident for SPEI time scales of 48 months. PC2 is clearly representative of the lower sectors of the Ebro River and several sub-basins of the Iberian mountains. Principal component 3 (PC3; 11% of the total variance) is characterized by a strong response of the SSI to intermediate time scales of the SPEI (6–10 months). The response to short time scales was very weak, and after month 11 the correlation coefficients decreased markedly. Few sub-basins had a strong correlation with PC3, with greater correlations occurring in some sub-basins in the lower reaches of the Ebro River (which also exhibited significant correlations with PC2) and in some sub-basins of the eastern Pyrenees.

Figure 7 shows box plots of the values of altitude, total area, percentage of area with a permeable substrate (limestones, sandstones, conglomerates, sands and gravels derived from a geologic map of the basin at a spatial scale of 1:100,000), and the impounded ratio index (Batalla et al., 2004) for those basins classified in each of the three categories according to the maximum loading rule. Sub-basins represented by PC1 are generally at higher altitudes and have less regulation by dams compared with sub-basins represented by the other two components. Sub-basins represented by PC2 are generally at lower altitudes than those represented by PC1, and have more regulation by dams and a higher percentage of their surface covered by permeable lithology. Basins represented by PC3 have the largest surface, a lower percentage of permeable substrate, a higher

level of the impoundment ratio index, and a very similar average altitude to those represented by PC2.

4.2 The response of the SSI to the monthly SPEI

A PCA based on monthly data identified seasonal behavior in the response of the SSI to the various time scales of the SPEI, and showed that seven PCs (PC1–PC7) explained 78% of the total variance. Figure 8 shows the PC scores in the form of contour plots, and Figure 9 shows the spatial distribution of the PC loadings.

PC1 (20% of the variance) was characterized by a response to short and medium time scales (1–8 months) during autumn. In winter, strong correlations were only observed at short time scales (1–3 months), and in spring the maximum correlations were found for medium time scales (3–6 months). The maximum correlation with PC1 was found in 22 sub-basins, which are mainly located in the westernmost part of the Ebro basin.

PC2 (15% of the variance) was characterized by the absence of a correlation between the SSI and the SPEI during summer, and strong correlations in winter and spring, especially at time scales of 2 to 5 months. Maximum correlation with PC2 was found for 25 sub-basins, which are mainly located in the westernmost part of the basin (Cantabrian mountains and the headwaters of the westernmost part of the Iberian mountains). PC2 also showed a strong correlation with some sub-basins located in the foothills of the central Pyrenees.

PC3 (15% of the total variance) was characterized by maximum correlation with the shortest time scales (1–3 months) in summer and early autumn. From November to March the maximum correlations shifted to longer time scales. In February the maximum correlation was found with SPEI time scales of 7 months, and the correlation

remained very strong until a time scale of 14 months. From March to June the maximum correlation occurred at a time scale of 7 months, and a decrease in the correlation with short time scales was particularly evident. This pattern was characteristic of headwaters in the central and eastern Pyrenees; 26 sub-basins showed maximum correlation with this component.

PC4 (9% of the variance) was characterized by strong and persistent correlations from short to long time scales during the period from May to October. In autumn and winter the correlations were noticeably less, particularly at short time scales (1–5 months). This component was strongly correlated with 13 sub-basins located mainly in the lower reaches of the Ebro River.

PC5 (9% of the total variance) was characterized by autumns with strong correlations at short time scales (1–3 months); the correlations rapidly decreased at longer time scales. In winter and early spring the correlations were progressively maintained at longer time scales (up to 8 months). In late spring and summer the correlations were very strong for all temporal scales considered (1–24 months). This component was highly correlated with four sub-basins located mainly in high altitude areas of the eastern Pyrenees.

PC6 and PC7 (6% and 5% of the total variance, respectively) were characterized by very weak (in some cases negative) correlations throughout most of the year. For PC6 the correlations were slightly negative for most of the year, although these were not statistically significant ($\alpha < 0.05$). Exceptions were the December–February period, when positive correlations were evident for time scales of 3–10 months, and in summer, when positive correlations were found for time scales > 10 months. In all cases the correlations were statistically significant. PC7 only showed statistically significant positive correlations in October for very short time scales, and in February and March

for most of the time scales. As occurred for PC6, the values of the coefficients of correlation were very low. PC6 and PC7 showed a maximum correlation with 5 and 3 sub-basins, respectively, with no clear geographical distribution.

Figure 10 shows box plots of the altitude, surface area, percentage of permeable substrate, and the impounded ratio index for those basins classified in any of the seven PCs according to the maximum loading rule.

The sub-basins represented by PC1 are general at low mean altitude, have a high percentage of surface with a permeable substrate and a low level of regulation by dams. The sub-basins represented by PC2 are at intermediate altitudes, have relatively high values of substrate permeability and one of the highest levels of impoundment. The sub-basins associated with PC3 and PC5 are at the highest mean altitudes, and have the lowest substrate permeability and very low levels of dam regulation. The sub-basins represented by PC4 have intermediate mean altitude and permeability, and generally a high level of regulation by dams. The sub-basins related to PC6 and PC7 in general have intermediate values for the three characteristics considered.

5. DISCUSSION

The results show that different sub-basins of the Ebro River basin responded in very different ways to precedent climatic conditions. Moreover, the response time of each drainage area varied markedly throughout the year and had contrasting seasonal patterns.

Three contrasting patterns were observed when continuous correlations were performed without considering monthly variability in the river regimes, and these showed a clear distribution in space along the Ebro basin. Thus, streamflow exhibited a major response

at short SPEI time scales (2–4 months) at a large number of gauging stations. In general, these sub-basins have a high mean altitude, are small in size, and predominantly have a permeable substrate and a low level of regulation by dams. These sub-basins are mostly located in the highest altitude areas of the Pyrenees and upstream of the main reservoirs, which are generally located in the mountain foothills and the main course of the Ebro River. All the characteristics of this group of sub-basins contribute to a rapid response of river flow to climatic conditions. Small and mountainous sub-basins general have short and steep water paths, which are generally associated with a fast hydrological response to precipitation events (Soulsby et al., 2006). The low percentage of permeable substrate suggests a minor role of groundwater storage, which has previously been identified as one of the major reasons for delays in the response times of basins (McGuire and McDonnell, 2006). In a previous study Soulsby et al. (2006) used tracers to quantify the stream water residence time in seven sub-basins of the Feshie catchment (Scotland; 230 km^2), and concluded that groundwater (which is determined by lithology and soil characteristics) was the main variable explaining flow path partitioning and residence times in the basin. In addition, sub-basins that respond to short time scales had minor influence of dam operations, able to delay the response time from several months to more than one year, depending on the water storage capacity and the dam operation strategies used (Vicente-Serrano and López-Moreno, 2005; López-Moreno et al., 2007, Lorenzo-Lacruz et al., 2010). Other sub-basins of the Ebro River exhibited a clearer correlation to longer time scales of the SPEI. The slowest response time (10–20 months) mainly corresponded to basins with a high percentage of surface covered by permeable substrate, particularly in sectors of the Iberian Mountains, where limestones are dominant and the role of groundwater circulation is consequently enhanced. Intermediate response times (6–10 months) were

characteristic of the lower sectors of the Ebro basin. Two explanations are possible for this observation. Firstly, the lowest reaches of the basin comprise tributaries associated with catchments of the two previous types and this is reflected in the hydrological response. Secondly, the lowest reaches of the Ebro basin have the greatest impounded ratio index. Previous studies have shown that most reservoirs in the Ebro basin have an annual rather than a pluri-annual management regime (Batalla et al., 2004), which explains why they may have a delayed response time to climatic conditions and a less intense response than groundwater storage.

When the response was analyzed on a monthly basis the patterns obtained were more complex and spatially less coherent. This is mainly because of the combined effects of the factors explaining the response time of particular sub-basins, the time of the year, and the large variability in climatic and hydrological seasonality in the study area (García-Ruiz et al., 2001; López and Justribó, 2010). However, a number of conclusions can be derived from the observed patterns and the spatial distribution of the monthly response time. For instance, sub-basins with a substantial cover of permeable rocks showed a generally lower relationship with SPEI, and normally at longer time-scales, as occurred in several months for PC6 and PC7. The sub-basins with a high level of river regulation by dams also showed a stronger relationship to longer time scales during some periods of the year; whereas the influence of immediately preceding climatic conditions on river flow variability was minimal at other times of the year. The effect of dam management on the response time of river flows was particularly evident in those sub-basins represented by PC2 and PC4. The sub-basins represented by PC2 are influenced by reservoirs located in the headwaters of the Ebro basin and the foothills of the Pyrenees. In these areas the reservoirs are of medium size (maximum 600 hm^3) and generally store water from autumn to spring. Depending on the previous climatic

conditions, managers of the reservoirs need to retain differing percentages of the water inflows, and hence every year release very different amounts of water to downstream areas (López-Moreno et al., 2004). This explains the strong correlations with long time scales of the SPEI in autumn and winter months. Water release from these dams during summer tends to be constant as a consequence of imposed ecological flows, and therefore the river flows in summer are not correlated with antecedent climatic conditions. In contrast, sub-basins represented by PC4 are affected by the largest reservoirs in the basin (up to 1000 hm^3), which are located in the lower reaches of the Ebro River. These reservoirs store a large proportion of the autumn and winter inflows (Batalla et al., 2004) and release constant outflows during this time of the year. This explains the weak response of the streamflow to previous climatic conditions. When these reservoirs have stored sufficient water to ensure supply during the period of high demand in late spring and summer, water is released downstream according to the inflows they receive, which in turn depends on the precedent climatic conditions. This explains the sudden increase in the correlation coefficients between the SSI and the SPEI during spring and summer.

In addition to lithology and the level of impoundment, snow is a key factor explaining the variability of the hydrological response time of sub-basins within the Ebro basin. PC3 and PC5 represent the sub-basins at higher altitudes, where snow would be expected to have the greatest influence. In both groups of sub-basins, which are located at high altitudes in the central and eastern Pyrenees, there was a progressive increase in the correlations at the longer time scales during winter, and particularly during spring. This is a consequence of the storage of winter precipitation as snow, and its subsequent contribution to streamflow during the snowmelt period (Adam et al., 2009). It has been previously demonstrated that recent evolution of spring runoff in the Pyrenees is not

determined by the climatic conditions in spring, but shows a clear relationship with temperature and precipitation during winter (López-Moreno and García-Ruiz, 2004).

The results of this study suggest the importance of quantifying the response time of streamflow to climatic conditions at various time scales, as this is an indicator of the sensitivity of sub-basins to their main environmental characteristics and the anthropogenic influences on natural streamflow variability (Dunn et al., 2007; McDonnell et al., 2010). Moreover, the SPEI (Vicente-Serrano et al., 2010) has been demonstrated to be a useful index for monitoring the interannual and seasonal variability of streamflow in basins with contrasting characteristics. Thus, an approach such as the one presented in this study will be very useful in identifying the optimum time scales at which to monitor climatic droughts to assess streamflow conditions in different regions and river stretches. Meanwhile, this approach offers an interesting additional indicator to classify large river basins in homogeneous regions. The results also have implications for understanding the ways in which changes in precipitation or evapotranspiration rates in particular seasons may differentially affect hydrological conditions in different sub-basins, even those in very close proximity. The results also suggest the need to identify the appropriate time scales for assessment of the antecedent climatic conditions in relation to the impacts of projected climate change on hydrology and water resources availability.

6. CONCLUSIONS

This study highlights the large spatial and seasonal variability of the hydrological response in the Ebro River basin to previous climatic conditions. Altitude, groundwater storage, dam operations and snowpack were found to be major factors affecting the

variety of river flow responses to climatic time scales. Generally, unregulated basins located in mountain areas (mainly in the Pyrenees) showed the strongest correlation to the SPEI calculated at the shortest time scales (2–4 months). In these areas the presence of snow produced marked seasonal differences, with longer response times during late winter and spring. Basins in areas where ground water reserves are more important (mainly in the Iberian system) maintained a strong correlation with the SPEI calculated at very long time scales (10–20 months). Sub-basins located downstream of the main reservoirs in the Ebro basin were most strongly correlated with the SPEI calculated at intermediate time scales (6–10 months). The management regime applied to the various reservoirs led to marked seasonal differences.

ACKNOWLEGMENTS

This study was supported by the research projects CGL2006-11619/HID, CGL2008-01189/BTE, and CGL2008-1083/CLI, financed by the Spanish Commission of Science and Technology, and FEDER, EUROGEOSS (FP7-ENV-2008-1-226487), ACQWA (FP7-ENV- 2008-1-212250) and the projects "La nieve en el Pirineo aragonés: Distribución espacial y su respuesta a las condiciones climáticas", financed by "Obra Social La Caixa", and "Influencia del cambio climático en el turismo de nieve-CTTP1/10", financed by the Comisión de Trabajo de los Pirineos, CTP.

References

Abramowitz, M. and Stegun, I.A., 1965. Handbook of Mathematical Functions. Dover Publications, New York.

Adam, J.C., Hamlet, A.F., Lettenmaier, D.P., 2009. Implications of global climate change for snowmelt hydrology in the 21st century. Hydrological Processes 23, 962-972.

Batalla, R.J.; Gómez, C.M. and Kondolf, M., 2004. Reservoir-induced hydrological changes in the Ebro River basin (NE Spain). Journal of Hydrology 290**,** 117-136.

Beven K.J., 2002. How far can we go in distributed hydrological modelling? Hydrology and Earth System Science 5, 1-12.

Dai, A., (2011): Characteristics and trends in various forms of the Palmer Drought Severity Index (PDSI) during 1900-2008. Journal of Geophysical Research-Atmosphere. doi:10.1029/2010JD015541.

Daly, C., Neilson, R.P. and Phillips, D.L., 1994. A statistical-topographical model for mapping climatological precipitation over mountainous terrain. J. Clim. Appl. Meteor. 33, 140-158.

Dunn, S.M., McDonnell, J.J., Vache, K.B., 2007. Factors influencing the residence time of catchment waters: a virtual experiment approach. Water Resources research 43: W06408.

Fleig, A.K., Tallaksen L.M., Hisdal, H., Hannah, D.M., 2011. Regional hydrological drought in north-western Europe: linking a new regional drought area index with weather types. Hydrological Processes 25, 1163-1179.

García-Ruiz, J.M., Beguería, S., López-Moreno, J.I., Lorente-Grima, A. y Seeger, M., 2001. *Los recursos hídricos superficiales del Pirineo aragonés y su evolución reciente*. Geoforma Ediciones, Logroño, 191 p.

García-Ruiz, J.M., Regüés, D., Alvera, B., Lana-Renault, N., Serrano-Muela, P., Nadal-Romero, E., Navas, A., Latron, J., Martí-Bono, C., Arnáez, J., 2008. Flood Generation and Sediment Transport in Experimental Catchments Affected By Land Use Changes In The Central Pyrenees. Journal of Hydrology, 356 (1-2), 245-260.

García-Ruiz J.M., López-Moreno, J.I. Serrano-Vicente S,M, Beguería, S., Lasanta, T., 2011. Mediterranean water resources in a global change scenario. Earth Science Reviews 105 (3-4), 121-139.

Gonzalez-Hidalgo J.C., Lopez-Bustins J.A., Stepánek, P., Martin-Vide J., De Luis, M., 2009. Monthly precipitation trends on the Mediterranean fringe of the Iberian Peninsula during the second-half of the twentieth century (1951-2000). International Journal of Climatolology 29 (10), 1415-1429.

Hosking, J.R.M., 1990. L-Moments: Analysis and estimation of distributions using linear combinations of order statistics. Journal of Royal Statistical Society B 52, 105-124.

Jollife, I.T., 1990. Principal component analysis: a beginner's guide. Part I: Introduction and application. Weather 45, 375-382.

Kenawy, A., López-Moreno, J.I., Stepanek, P., M.Vicente-Serrano, S. (in press). An assessment of the role of homogenization protocols in the performance of daily temperature series and trends: application to Northeastern Spain. International Journal of Climatology. DOI: 10.1002/joc.3410

Kroll, C.N., and Vogel, R.M., 2002. Probability distribution of low streamflow series in the United States. Journal of Hydrologic Engineering 7: 137-146.

Latron, J., Gallart, F. 2008. Runoff Generation Processes In A Small Mediterranean Research Catchment (Vallcebre, Eastern Pyrenees). Journal of Hydrology 358, 206-220.

López-Moreno, J.I. and García-Ruiz, J.M., 2004. Influence of snow accumulation and snowmelt on streamflow in the Central Spanish Pyrenees. International Journal of Hydrological Sciences 49 (5), 787-802.

López-Moreno, J.I., Beguería, S. and García-Ruiz, J.M., 2004. The management of a large mediterranean reservoir: storage regimes of the Yesa reservoir, Upper Aragón River basin, Central Spanish Pyrenees. Environmental Management 34 (4), 508-515.

López-Moreno, J.I., Beguería, S., Vicente-Serrano, S.M. and García-Ruiz, J.M., 2007. The influence of extreme phases of the North Atlantic Oscillation on water resources of the Tagus river basin (Spain): precipitation, stream flow anomalies, and reservoir management strategies. Water Resources Research 43, W09411.

López-Moreno, J.I., Vicente-Serrano, S.M., Moran-Tejeda, E. Zabalza, J., Lorenzo-Lacruz, J., García-Ruiz, J.M., 2011. Impact of climate evolution and land use changes on water yield in the Ebro basin. Hydrology and Earth System Science 15, 311-322.

López, R., Justribó, C., 2010. The hydrological significance of mountains: a regional case study, the Ebro River basin, northeast Iberian Peninsula. Hydrological Sciences Journal, 55 (2), 223–233, 2010.

Lorenzo-Lacruz, J., Vicente-Serrano, S.M., López-Moreno J.I., Beguería, S., Cuadrat, J.M., García-Ruiz, J.M., 2010. The impact of droughts and water management on

various hydrological systems in the headwaters of the Tagus River (central Spain). Journal of Hydrology 386(1-4), 13-26.

Ninyerola, M., Pons, X., Roure J.M., 2007. Objective air temperature mapping for the Iberian Peninsula using spatial interpolation and GIS. International Journal of Climatology 27 (9), 1231-1242.

McDonnell, J.J., McGuire, K., Aggarwall, P., Beven, K.J., Biondi, D., Destouni, G., Dunn, S., James, A., Kirchner, J., Kraft, P., Lyon, S., Maloszewski, P., Newman, B., Pfister, L., Rinaldo, A., Rodhe, A., Sayama, T., Seibert, J., Solomon, K., Soulsby, C., Stewart, M., Tetzlaff, D., Tobin, D., Troch, P., Weiler, M., Western, A., Wörman, A., Wrede, S., 2010. How old is streamwater? Open questions in catchment transit time conceptualization, modelling and analysis. Hydrological Processes 24, 1745-1754.

McGuire, K., McDonnell, J.J., 2006. A review and evaluation of catchment transit time modeling. Journal of Hydrology 330, 543-563.

McKee, T.B.N., Doesken, J. and J. Kleist, 1993. The relationship of drought frecuency and duration to time scales. Eight Conference on Applied Climatology. Anaheim, CA, Amer. Meteor. Soc. 179-184.

McKee, T.B.N., Doesken, J. and J. Kleist, J., 1995. Drought monitoring with multiple time scales. Ninth Conference on Applied Climatology, Dallas, TX, Amer. Meteor. Soc., 233-236.

Post, D.A., Jakeman, A.J., 1996. Relationships between catchment attributes and hydrological response characteristics in small Australian mountain ash catchments. Hydrological Processes 10, 877-892.

Richman, M.B., 1986. Rotation of Principal Components. Journal of Climatology 6, 29-35.

Soulsby, C., Tetzlaff, D., Rodgers, P., Dunn, S., Waldron, S., 2006. Runoff processes, stream water residence times and controlling landscape characteristics in a mesoscale catchment: An initial evaluation. Journal of Hydrology 325, 197-221.

Tallaksen, L.M., 1995. A review of baseflow recession analysis. Journal of Hydrology 165, 349-370.

Thornthwaite, C.W., 1948. An approach toward a rational classification of climate. Geographical Review, 38, 55-94.

Van der Schrier, G., Jones, P.D., Briffa, K.R. 2011. The sensitivity of the PDSI to the Thornthwaite and Penman□Monteith parameterizations for potential evapotranspiration, J. Geophys. Res., 116, D03106, doi:10.1029/2010JD015001.

Vicente-Serrano S. and López-Moreno, J.I., 2005. Hydrological response to different time scales of climatological drought: an evaluation of the standardized precipitation index. Hydrology and Earth System Sciences 9, 523-533.

Vicente-Serrano, S.M., Beguería, S., López-Moreno, J.I., 2010. A multi-scalar drought index sensitive to global warming: the standardized precipitation evapotranspiration index SPEI. Journal of Climate 23, 1696-1718.

Vicente-Serrano, S.M., López-Moreno, J.I., Beguería, S., Lorenzo-Lacruz, J., Azorin-Molina, C., Morán-Tejeda, E. (2011). Accurate computation of a streamflow drought index. Journal of Hydrologic Engineering. doi:10.1061/(ASCE)HE.1943-5584.0000433.

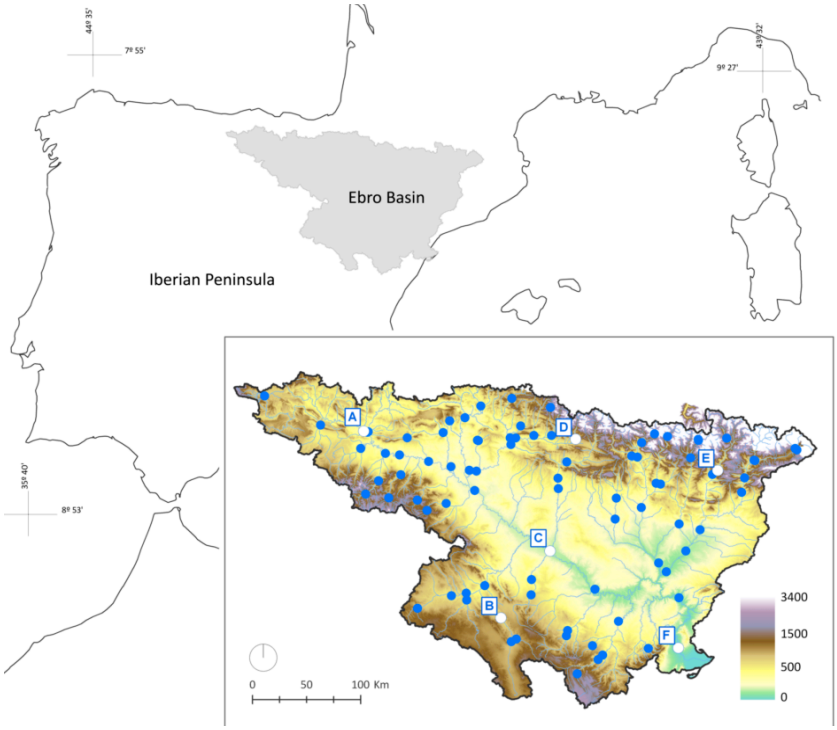

Figure 1. Study area. The blue dots are the gauging stations, and the letters indicate the gauging stations shown in Figure 2.

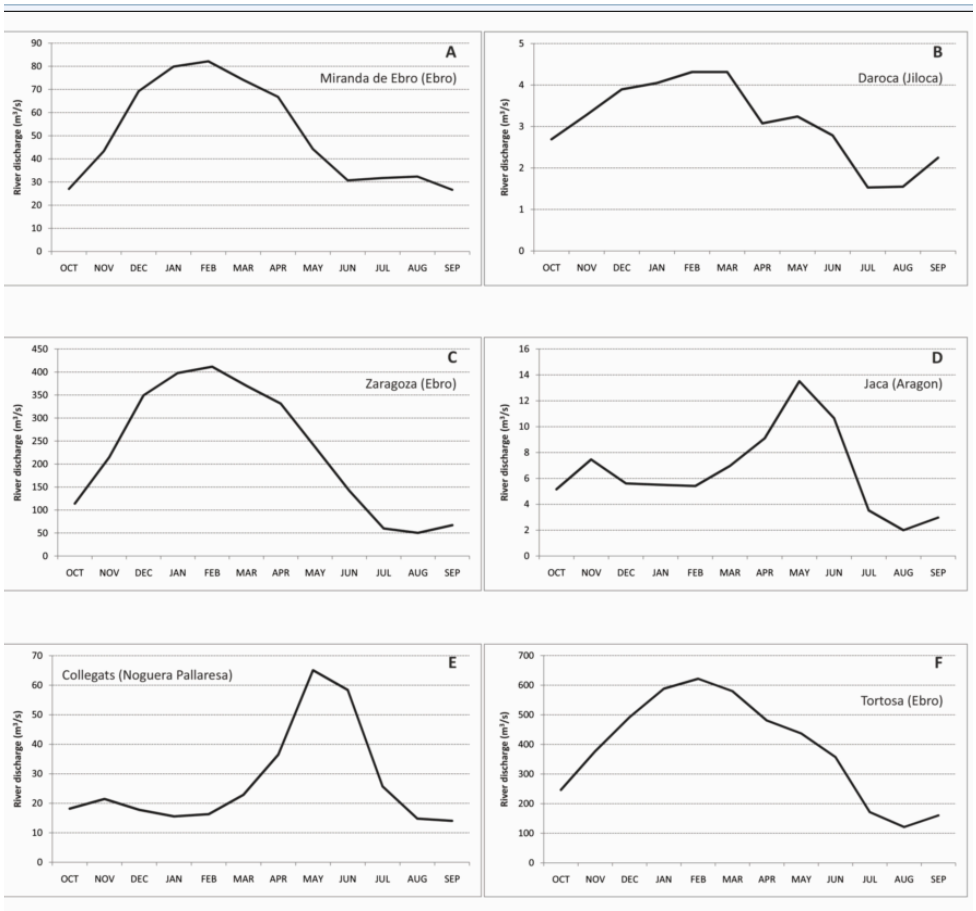

Figure 2. Monthly river discharge in six selected gauging stations within the Ebro basin. The location of the stations are as shown in Figure 1.

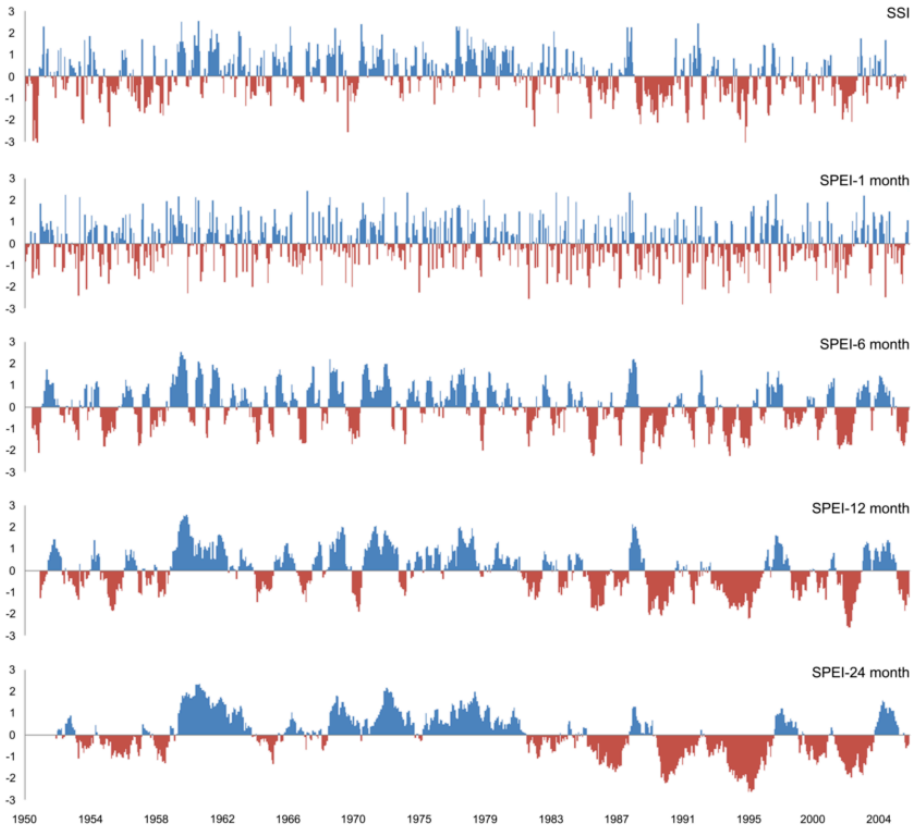

Figure 3. The SSI calculated from the monthly river discharge series for the Ebro River in Zaragoza. The SPEI was calculated for the drainage area of the gauging station at 1, 6, 12 and 24 months.

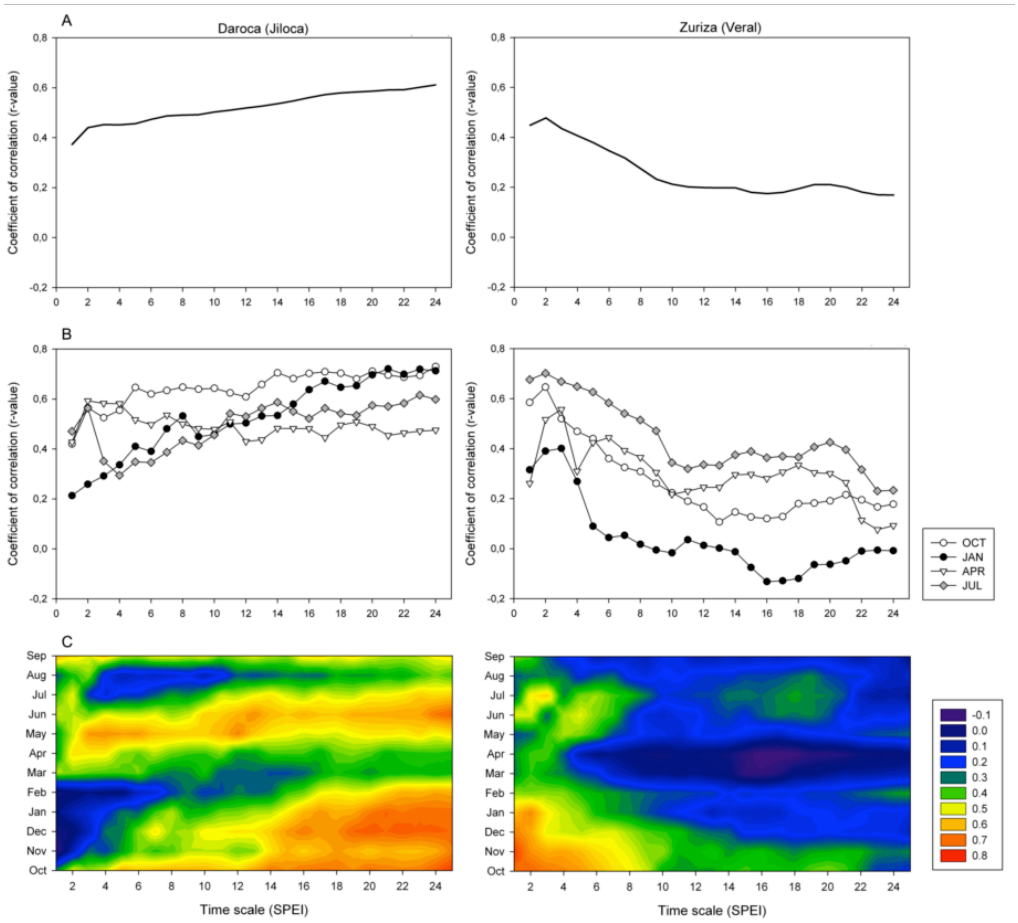

Figure 4. A) Correlation coefficients between continuous series of the SSI and the SPEI at different time scales for the Jiloca River at Daroca (left) and the Veral River at Zuriza (right). B) Correlation coefficients between the SSI and the SPEI at different time scales for the Jiloca River at Daroca (left) and the Veral River at Zuriza (right) for the SSI series for October, January, April and July. C) Contour plots that summarize the correlation coefficients for the 12 months of the year.

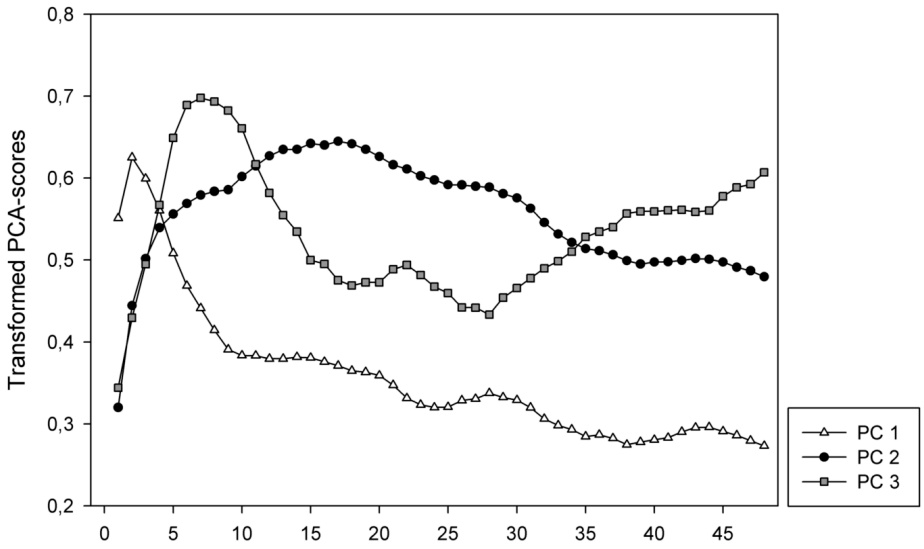

Figure 5. Patterns of response of the SSI to various time scales of the SPEI discriminated by principal component analysis (PCA; Varimax rotation). The PCA scores were transformed to the original units (r-values), which were obtained by weighting the scores by the coefficients of the factorial punctuation matrix.

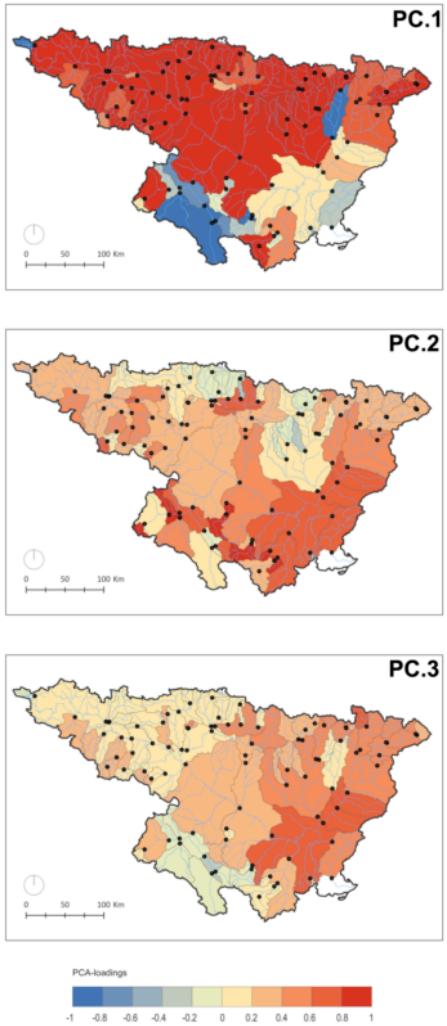

Figure 6. Spatial distribution of the principal component analysis loadings corresponding to the three extracted principal components represented in Figure 5.

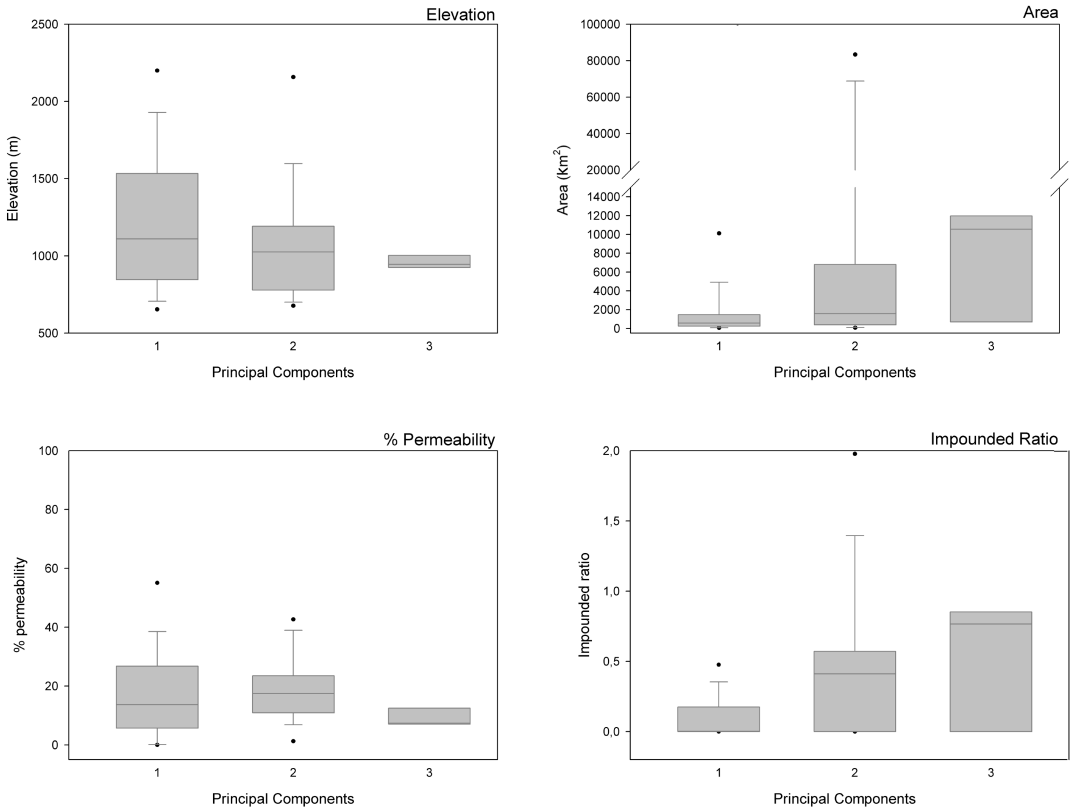

Figure 7. Box plots for altitude, surface area, percentage of area with a permeable substrate, and the impounded ratio index for those basins represented by each of the three principal components. The line is the mean, the boxes indicate the 25th and 75th percentiles, the bars are the 10th and 90th percentiles, and the dots are the 5th and 95th percentiles.

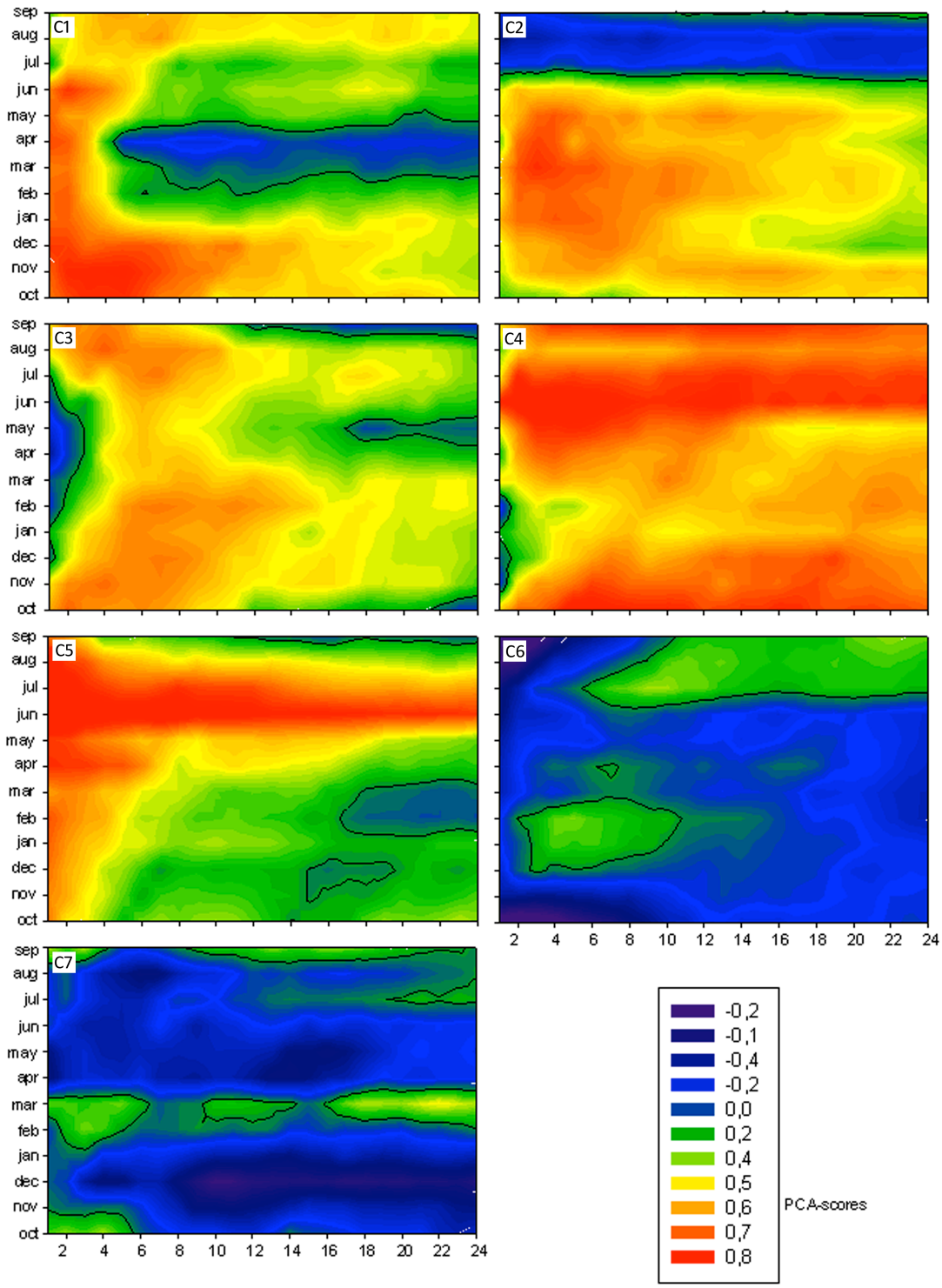

Figure 8. Patterns of monthly response of the SSI to various SPEI time scales discriminated by principal component analysis (PCA; Varimax rotation). The PCA

scores are shown in the r-values of the original varible, which were obtained by weighting the original variables by the coefficients of the factorial punctuation matrix.

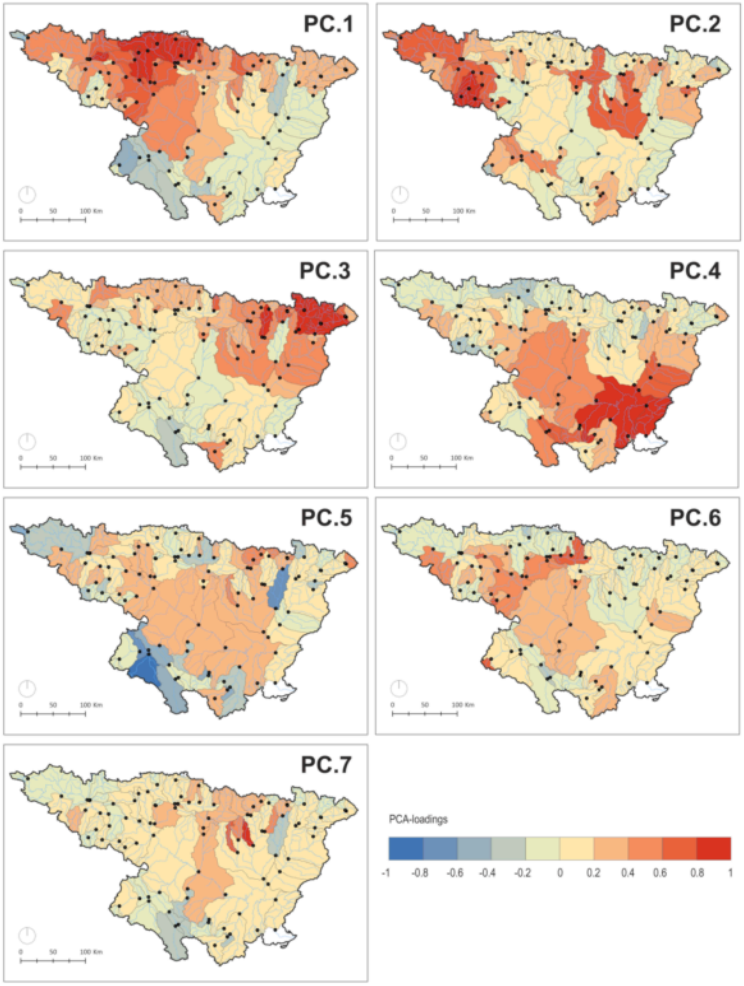

Figure 9. Spatial distribution of the principal component analysis loadings corresponding to the seven extracted principal components represented in Figure 8.

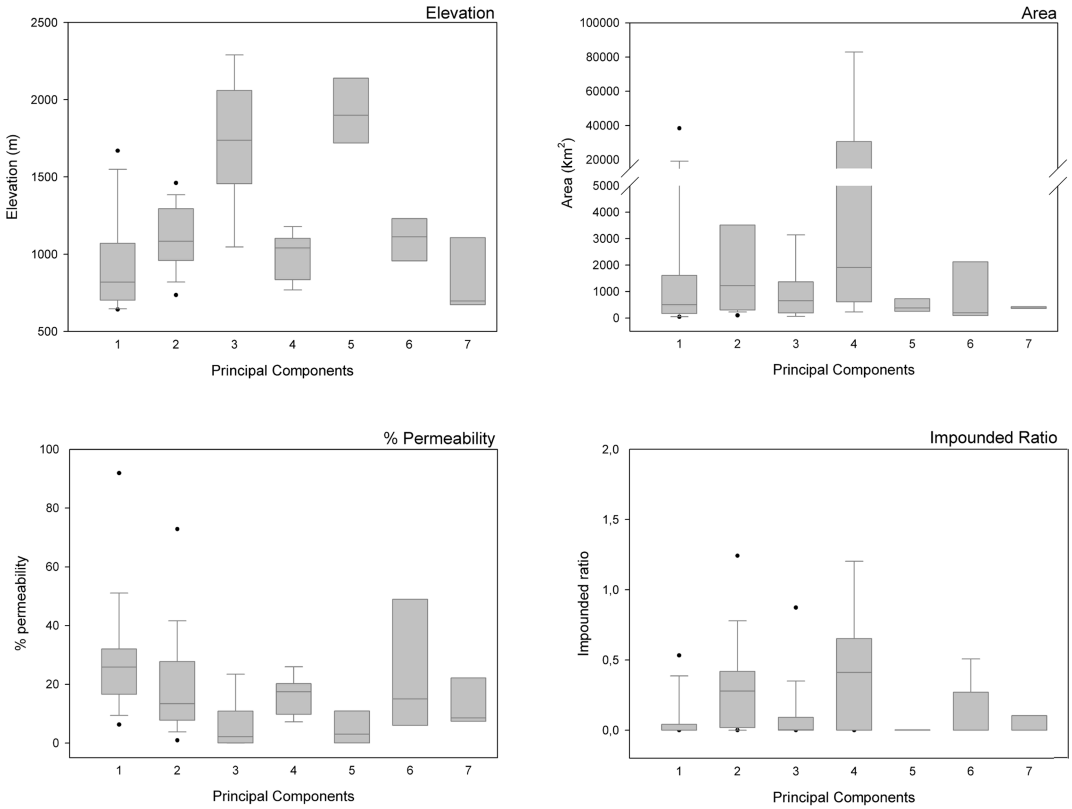

Figure 10. Box plots of altitude, surface area, percentage of area with a permeable substrate, and the impounded ratio index of those basins represented by each of the seven principal components. The line is the mean, the boxes indicate the 25th and 75th percentile, the bars indicate the 10th and 90th percentiles, and the dots indicate the 5th and 95th percentiles.